Amplitude Malformation in the IFFT Ocean Wave Rendering under the Influence of the Fourier Coefficient

Lining Chen, Yicheng Jin, and Yong Yin

Abstract—Although Tessendorf's IFFT Gerstner wave model has been widely used, the value of *A*, a constant of the Fourier coefficient, is not given. *A* will strongly influence the shape of the rendered ocean wave and even cause amplitude malformation. We study the algorithm of the IFFT Gerstner wave, and give the method of *A* calculating. The method of the paper can guarantee there is no amplitude malformation in rendered ocean waves. The expression of the IFFT Gerstner wave with the amplitude of the cosine wave is derived again. The definite integral of the wave number spectrum is discretized. Further, another expression of the IFFT Gerstner wave is gotten. The Fourier coefficient of the expression contains the wave number spectrum and the area of the discrete integral domain. The method makes the shape of the generated wave stable. Comparing Tessdendorf's method with the method of the paper, we find that the expression of *A* should contain the area of the discrete integral domain and the spectral constant of the wave number spectrum. If *A* contains only the spectral constant, the amplitude malformation may occur. By reading some well known open source codes, we find that the code authors adopted some factitious methods to suppress the malformed amplitude Obviously, the code authors have already noticed the phenomenon of the malformation, but not probed the cause. The rendering results of the codes are close to that of the method of the paper. Furthermore, the wave potential is computed using the Gerstner wave model directly, the author find it is quite close to that of the paper. The experimental results and comparisons show that the method of the paper correctly computes the wave potential and effectively solves the problem of amplitude malformation.

Index Terms—Gerstner wave, IFFT, ocean wave spectrum, Riemann sum.

Lining Chen is with the Laboratory of Marine Dynamic Simulation & Control, Dalian Maritime University, Dalian, China 116023 (phone: 0086-15998558716, e-mail: chenlining19811011@hotmail.com)

Yicheng Jin is with the Laboratory of Marine Dynamic Simulation & Control, Dalian Maritime University, Dalian, China 116023 (phone: 0086-041184727197, e-mail: jycdmu@dlmu.edu.cn)

Yong Yin is with the Laboratory of Marine Dynamic Simulation & Control, Dalian Maritime University, Dalian, China 116023 (phone: 0086-041184729651, e-mail: bushyin_dmu@263.net)

I. INTRODUCTION

THE reproduction of the ocean wave is an important and challenging research topic in computer graphics. Many fields of activity rely on it: virtual reality, movies, games, maritime simulators and so on.

Bruce [1] and Nelson [2] linearly summed cosine waves to reproduct the height field of the sea surface. The rendered ocean wave is linear and regular. However, the real ocean wave is nonlinear and irregular [3]. To get more realistic results, researchers began to employ nonlinear methods. The Gerstner wave is an exact nonlinear solution for waves of finite amplitude on deep water [4], and is widely applied in ocean wave simulation. Fourier et al [5] introduced the Gerstner wave to ocean wave rendering, and added the random phase shift in the model. So the rendered wave is irregular as well as nonlinear. Thon et al [6] and Fréchot [7] applied the directional spectrum in the Gerstner wave model. The directional spectrum is gotten through observation, so the works of [6, 7] combined the observational oceanographic data with the Gerstner wave model. Consequently, the approaches of [6, 7] are also named as "hybrid approaches" [8]. The geometry of the sea surface can be optimized by some approaches, such as the adaptive surface mesh [9], the quad tree [10], the real-time adapting mesh [11], and the fractal reconciliation [12]. The Perlin noise [6, 13] was added to the height field as random disturbance. Additionally, Prachumrak et al [14] realized the interaction between the floating object and the sea surface.

The direct usage of the Gerstner wave, as mentioned above, is very convenient. However, if a lot of cosine waves are involved, the summation becomes expensive. A cheaper alternative exists by way of IFFT [15], i.e. the IFFT Gerstner wave. IFFT has a large degree of parallelism in each stage of the computation [16] and its implementation is efficiently speeded up by GPU [17]. Tessendorf [18] is the pioneer of applying the IFFT Gerstner wave model in graphics. The Fourier coefficient of Tessendorf's method contains the wave number spectrum and random numbers, so the generated wave is irregular and nonlinear. The optimizing approach for the geometry included the concentric circle grid [19] and clipmap [20]. By the optimization, the mesh of the geometry is refined or coarsened according to the eye position. Mitchell [21] and Miandji et al [22] utilized image processing algorithms to increase the resolution of the sampled height map.

Swierkowski et al [23] generated the ship wave on the IFFT sea surface. Weerasinghe et al [24] combined the IFFT Gerstner wave with 6-DOF (degree of freedom) ship motion model. The Perlin noise [25], and the high frequency data [26] can also add to the IFFT sea surface. What is more, the model of the IFFT Gerstner wave was also used to create the special effects, such as splashing [27, 28], the whitecap [29] and the foam [30].

To facilitate reading, some parameters and symbols are defined here. We use Ψ to denote the wave number spectrum, and A_Ψ the spectral constant of the corresponding wave number spectrum. $A_{\Psi,Ph}$ is the spectral constant of the Phillips spectrum, $A_{\Psi,PM}$ is that of Ψ_{PM} in expression (32), and $A_{\Psi,J}$ is that of Ψ_J in expression (33). A represents the numeric constant of the Phillips spectrum in expression (4).

The IFFT Gerstner wave was raised in [18], and [19-30] directly made use of it. All of them achieved satisfactory results. A is a numeric constant of the Phillips spectrum which is included in the expression of the Fourier coefficient, so A is also contained in the expression of the Fourier coefficient. Although Tessendorf's method has been widely used and studied, the author finds the value of A is not given in [18-30]. However, A strongly influences the shape of the generated ocean wave. If the expression of A contains only $A_{\Psi,Ph}$, the amplitude malformation may occur. The larger the area of the sea surface, the more serious the amplitude malformation. So the author thinks that the method of A calculating should be considered and provided.

The paper studies the model of the IFFT Gerstner wave, and gives the method of A calculating. The expression of the IFFT Gerstner wave with the amplitude of the cosine wave is derived again. To begin with, we discretize the definite integral of the wave number spectrum with the right Riemann sum. The area of the discrete integral domain depends on the sample mode for the wave number vector. Further, we can get an expression of the IFFT Gerstner wave. The Fourier coefficient of the expression contains the wave number spectrum and the area of the discrete integral domain of the sampled wave number vector. Comparison shows that the expression of A should include the spectral constant of the wave number spectrum as well as the discrete integral domain. Till now, a confusing problem is brought. Since A is not given, how did [18-30] get good rendering results? The author infers that some factitious methods may be taken to treat the amplitude malformation. The first method is setting A very small. Although [18-30] shared the same method and wave number spectrum, i.e. the Phillips spectrum, A, the numeric constant of the spectrum, is not given. So the user of the method in [18] can set A very small to treat the amplitude malformation. The second method is to multiply the height field by a small factor. After reading three widely used open source codes, osgOcean [31], oceanFFT [32] and fftrefraction [33], the author finds that the code authors adopt the factitious methods. This confirms the author's inference. The factitious method is effective but lack of basis. When compute the wave potential of the method of directly using the Gerstner wave model, we find the computed wave potential is close to that of the method of the paper. The comparisons and experiments results prove that the method of the paper correctly computes the wave potential, and effectively solves the problem of amplitude malformation.

II. PROBLEM STATEMENT

The model of the IFFT Gerstner wave [18] is expressed as:

$$\begin{cases} h(\vec{x}_{pq},t) = \sum_{\vec{k}_{ij}} \tilde{h}(\vec{k}_{ij},t)\exp(\sqrt{-1}\vec{k}_{ij}\cdot\vec{x}_{pq}), \\ \mathbf{D}(\vec{x}_{pq},t) = \sum_{\vec{k}_{ij}} -\frac{\vec{k}_{ij}}{k}\tilde{h}(\vec{k}_{ij},t)\exp(\sqrt{-1}\vec{k}_{ij}\cdot\vec{x}_{pq}). \end{cases} \quad (1)$$

where h is the elevation of the sea surface,

$\vec{x}_{pq}$ is the horizontal position, $\vec{x}_{pq} = (x_p, y_q) = (Lp/n, Lq/n)$,

t is the time,

$\tilde{h}$ is the Fourier coefficient,

$\vec{k}_{ij}$ is the wave number vector, $\vec{k}_{ij} = (k_{x,i}, k_{y,j}) = (2\pi i/L, 2\pi j/L)$, and $k = \|\vec{k}_{ij}\|$,

L is the width of the rendered ocean wave surface,

p, q, i and j are integers, and $-n/2 \le p,q, i,j < n/2$,

n is a positive integer, $n = 2^m$, and m is a positive integer,

$\sqrt{-1}$ is the imaginary unit, i.e. $(\sqrt{-1})^2 = -1$,

$\mathbf{D}$ is the choppy wave vector.

So the 3D coordinate of a point on the sea surface is $(\vec{x}_{pq} + \lambda\mathbf{D}(\vec{x}_{pq},t), h(\vec{x}_{pq},t))$. $\tilde{h}$ is expressed as:

$$\begin{aligned} \tilde{h}(\vec{k}_{ij},t) &= \tilde{h}_0(\vec{k}_{ij})\exp(\sqrt{-1}\omega_k t) \\ &+ \tilde{h}_0^*(-\vec{k}_{ij})\exp(-\sqrt{-1}\omega_k t). \end{aligned} \quad (2)$$

where $*$ is the notation for the complex conjugate, ω_k is the circular frequency, and $\tilde{h}_0$ is expressed as:

$$\tilde{h}_0(\vec{k}_{ij}) = \frac{1}{\sqrt{2}}(\varepsilon_1 + \sqrt{-1}\varepsilon_2)\sqrt{\Psi_{Ph}(\vec{k}_{ij})}. \quad (3)$$

where ε_1 and ε_2 are independent Gaussian random numbers. E and Var denote the expectation and variance respectively. $E(\varepsilon_1)=E(\varepsilon_2)=0$, and $Var(\varepsilon_1)=Var(\varepsilon_2)=1$. And Ψ_{Ph} is the Phillips spectrum, expressed as:

$$\Psi_{Ph}(\vec{k}) = A\frac{1}{k^4}\exp\left(-\frac{g^2}{U^4 k^2}\right)\cos^2(\theta - \alpha). \quad (4)$$

where A is a numeric constant, U is the wind velocity, and α is the angle between the wind direction and x axis. $\Psi_{Ph}(\vec{k})$ is in the spectral form raised in [34], i.e.

$\Psi_{Ph}(\vec{k}) \square k^{-4} f(\theta)$. But neither [34] nor [18-30] worked out the value of A . The author analyzed the structure of $\Psi_{Ph}(\vec{k})$, and found its frequency spectrum is similar to the P-M spectrum in form. If the Phillips and P-M spectra share the same wave potential, $A_{\Psi,Ph} = 3.48 \times 10^{-3}$, and U should be the wind velocity at the height of 19.5 m above the sea surface, i.e. $U_{19.5}$ [35]. Yet when the author applies $A = A_{\Psi,Ph}$ in rendering, the shape of the generated ocean wave is not stable. Figure 1 demonstrates the rendering results. The amplitudes of the waves in both Figure 1(a) and (b) are overlarge, and the bigger the width L is, the more serious the malformation is. So the author thinks that the method in [18] need re-examined, and the method of A calculating should be provided.
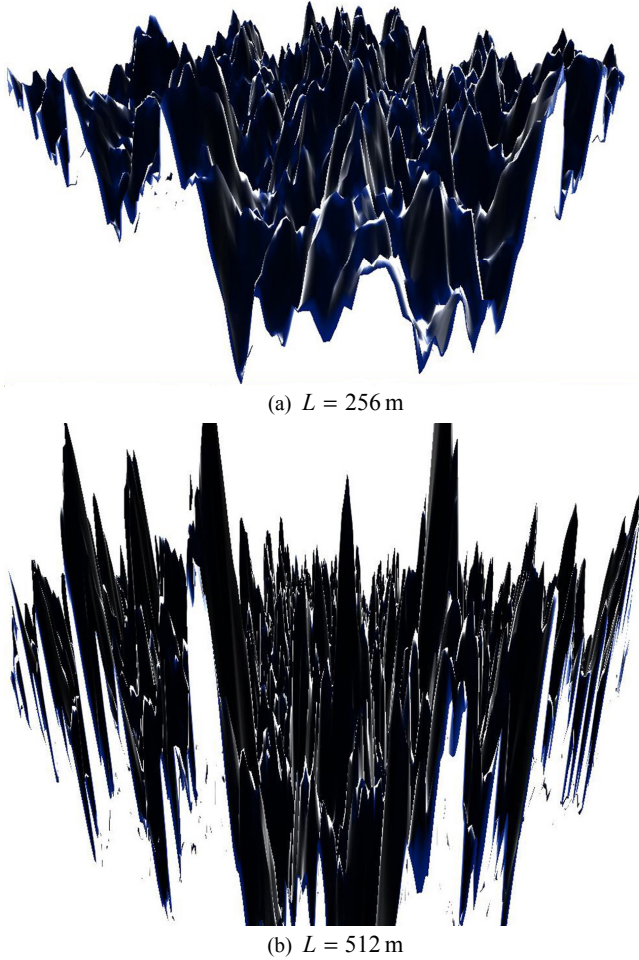

(a) $L = 256\,\mathrm{m}$

(b) $L = 512\,\mathrm{m}$

Fig. 1. The generated ocean waves of $\Psi_{Ph}(\vec{k})$ ($U_{19.5} = 10.0\,\mathrm{m/s}$).

III. THE IFFT GERSTNER WAVE

[18] provided the expression of the IFFT Gerstner wave, and [19-30] directly made use of it. However, neither [18] nor [19-30] gave the derivation of the expression. Although [15]

derived the expression of the IFFT Gerstner wave, the work was not complete and had some flaws:

- The IFFT solution of the height field was worked out but lack of some intermediate steps.
- The IFFT solution of the choppy wave was not produced.
- The expression of calculating the amplitude of the cosine wave is not provided.

To solve the flaws, the author need derive the expression of the IFFT Gerstner wave again, and then compare the re-derived expression with the expression of [18].

A. The IFFT Gerstner Wave with the Amplitude of the Cosine Wave

We now build the solution of the height field from a collection of real cosine waves:

$$h(\vec{x},t) = \sum_{i,j} A_{ij} \cos(\vec{k} \cdot \vec{x} - \omega_k t + \varphi_{ij}). \tag{5}$$

where φ_{ij} is the phase shift, and φ_{ij} is an independent uniform random number from $[0, 2\pi]$. Next we write the cosine in terms of complex exponentials:

$$\begin{aligned}
h(\vec{x}_{pq},t) = \sum_{i=-n/2+1}^{n/2-1} \sum_{j=-n/2+1}^{n/2-1} &\frac{1}{2}\exp[\sqrt{-1}(\vec{x}_{pq} \cdot \vec{k}_{ij})]A_{ij} \\
&\times \exp[\sqrt{-1}(\varphi_{ij} - \omega_k t)] \\
&+ \frac{1}{2}\exp[-\sqrt{-1}(\vec{x}_{pq} \cdot \vec{k}_{ij})]A_{ij} \\
&\times \exp[\sqrt{-1}(\omega_k t - \varphi_{ij})].
\end{aligned} \tag{6}$$

We write the cosine in terms of another complex exponentials:

$$\begin{aligned}
h(\vec{x}_{pq},t) = \sum_{i=-n/2+1}^{n/2-1} \sum_{j=-n/2+1}^{n/2-1} &\frac{1}{2}\exp[\sqrt{-1}(\vec{x}_{pq} \cdot \vec{k}_{-i,-j})]A_{-i,-j} \\
&\times \exp[\sqrt{-1}(\varphi_{-i,-j} - \omega_k t)] \\
&+ \frac{1}{2}\exp[-\sqrt{-1}(\vec{x}_{pq} \cdot \vec{k}_{-i,-j})]A_{-i,-j} \\
&\times \exp[\sqrt{-1}(\omega_k t - \varphi_{-i,-j})].
\end{aligned} \tag{7}$$

where $\vec{k}_{-i,-j} = -\vec{k}_{ij}$. By comparing expression (6) with (7), we can get the IFFT formula of the height field as:

$$h(\vec{x}_{pq},t) = \sum_{i=-n/2+1}^{n/2-1} \sum_{j=-n/2+1}^{n/2-1} \tilde{h}(\vec{k}_{ij},t)\exp[\sqrt{-1}(\vec{x}_{pq} \cdot \vec{k}_{ij})]. \tag{8}$$

where $\tilde{h}(\vec{k}_{ij},t)$ is the Fourier coefficient. It is expressed as:

$$\begin{aligned}
\tilde{h}(\vec{k}_{ij},t) = &\tilde{h}_0(\vec{k}_{ij})\exp(-\sqrt{-1}\omega_k t) \\
&+ \tilde{h}_0^*(-\vec{k}_{ij})\exp(\sqrt{-1}\omega_k t).
\end{aligned} \tag{9}$$

$\tilde{h}_0(\vec{k}_{ij})$ is express as:

$$\tilde{h}_0(\vec{k}_{ij}) = \frac{1}{2}(\cos\varphi_{ij} + \sqrt{-1}\sin\varphi_{ij})A_{ij}. \qquad (10)$$

We note $\tilde{h}_0(\vec{k}_{ij})$ includes A_{ij}. Therefore, $\tilde{h}(\vec{k}_{ij},t)$ contains A_{ij}. The above derived IFFT formula of the height field agrees well with that of [15].

The choppy wave is computed as:

$$\mathbf{D}(\vec{x}_{pq},t) =$$
$$-\sum_{i=-n/2+1}^{n/2-1}\sum_{j=-n/2+1}^{n/2-1}\frac{\vec{k}_{ij}}{k}A_{ij}\sin(\vec{k}_{ij}\cdot\vec{x}_{pq}-\omega_k t+\varphi_{ij}). \qquad (11)$$

The IFFT formula of the choppy wave is:

$$\mathbf{D}(\vec{x}_{pq},t) =$$
$$-\sum_{i=-n/2+1}^{n/2-1}\sum_{j=-n/2+1}^{n/2-1}\frac{\vec{k}_{ij}}{k}\tilde{h}_c(\vec{k}_{ij},t)\exp[\sqrt{-1}(\vec{k}_{ij}\cdot\vec{x}_{pq})]. \qquad (12)$$

$\tilde{h}_c(\vec{k}_{ij},t)$ is the Fourier coefficient of the choppy wave:

$$\tilde{h}_c(\vec{k}_{ij},t)=\tilde{h}_{c0}(\vec{k}_{ij})\exp(-\sqrt{-1}\omega_k t)$$
$$+\tilde{h}_{c0}^*(-\vec{k}_{ij})\exp(\sqrt{-1}\omega_k t). \qquad (13)$$

where $\tilde{h}_{c0}(\vec{k}_{ij})$ is defined as;

$$\tilde{h}_{c0}(\vec{k}_{ij}) = (\cos\varphi_{ij} + \sqrt{-1}\sin\varphi_{ij})\frac{A_{ij}}{2\sqrt{-1}}. \qquad (14)$$

So $\tilde{h}_c(\vec{k}_{ij},t)$ also contains A_{ij}.

B. Approximate Solution of the Amplitude of the Cosine Wave

The relation between the wave number spectrum and the amplitude of the cosine wave is as [36]:

$$\Psi(\vec{k}) = \sum_{i,j}\frac{A_{ij}^2}{2}\delta(\vec{k}-\vec{k}_{ij}). \qquad (15)$$

where δ denotes the Dirac function. $\Psi(\vec{k})$ is nonnegative, continuous, bounded, and derivable. One should note that $\Psi(\vec{k})$ represents the wave number spectrum, not only the Phillips spectrum.

The relation among $\mathrm{Var}(h)$, A_{ij} and $\Psi(\vec{k})$ is specialized as [36]:

$$\mathrm{Var}(h) = \frac{1}{2}\sum_{i,j}A_{ij}^2 = \iint_{\vec{k}}\Psi(\vec{k})\mathbf{d}\vec{k}. \qquad (16)$$

where $\mathbf{d}\vec{k}=\mathrm{d}k_x\mathrm{d}k_y = k\mathrm{d}k\mathrm{d}\theta$. Although expression (15) explains the relation between $\Psi(\vec{k})$ and A_{ij}, it is very difficult to be implemented by the computer. To facilitate the computer programming, we need another expression. Accordingly, we discretize $\iint_{\vec{k}}\Psi(\vec{k})\mathbf{d}\vec{k}$ to get the approximate solution of A_{ij}. The boundary value of the discrete integral domain is determined by the sample mode for the wave number

vector in IFFT. The generally used method of the discretization of the definite integral includes the Riemann sums, Trapezoid rule and Simpson rule [37]. We employ the right Riemann sum as:

$$\iint_{\vec{k}}\Psi(\vec{k})\,\mathbf{d}\vec{k} \approx \sum_{i,j}\Psi(\vec{k}_{ij})\Delta\mathrm{s}_{\vec{k}}. \qquad (17)$$

where $\Delta\mathrm{s}_{\vec{k}}$ is the area of the discrete integral domain. Let D_{ij} be the discrete integral domain, and $D_{ij}=\{(k_x,k_y)\,|\,k_x\in[k_{x,i-1},k_{x,i}], k_y\in[k_{y,j-1},k_{y,j}]\}$. Consequently, $\Delta\mathrm{s}_{\vec{k}} = \Delta k_x\Delta k_y$, and $\Delta k_x = k_{x,i}-k_{x,i-1} = \Delta k_y = k_{y,j}-k_{y,j-1} = 2\pi/L$. Now we work out the approximate solution of A_{ij} as:

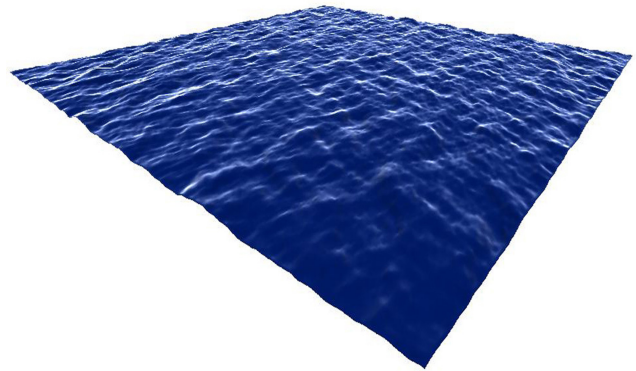$$A_{ij} = \sqrt{2\Delta\mathrm{s}_{\vec{k}}\,\Psi(\vec{k}_{ij})}. \qquad (18)$$

If $\Delta k_x,\Delta k_y \rightarrow 0$, expression (18) turns to expression (15). Now we get $\tilde{h}_0(\vec{k}_{ij})$ and $\tilde{h}_{c0}(\vec{k}_{ij})$ expressed as:

$$\begin{cases}\tilde{h}_0(\vec{k}_{ij}) = (\cos\varphi_{ij} + \sqrt{-1}\sin\varphi_{ij})\sqrt{\dfrac{\Delta\mathrm{s}_{\vec{k}}}{2}\Psi(\vec{k}_{ij})}, \\[3mm] \tilde{h}_{c0}(\vec{k}_{ij}) = \dfrac{1}{\sqrt{-1}}(\cos\varphi_{ij} + \sqrt{-1}\sin\varphi_{ij})\sqrt{\dfrac{\Delta\mathrm{s}_{\vec{k}}}{2}\Psi(\vec{k}_{ij})}.\end{cases} \qquad (19)$$
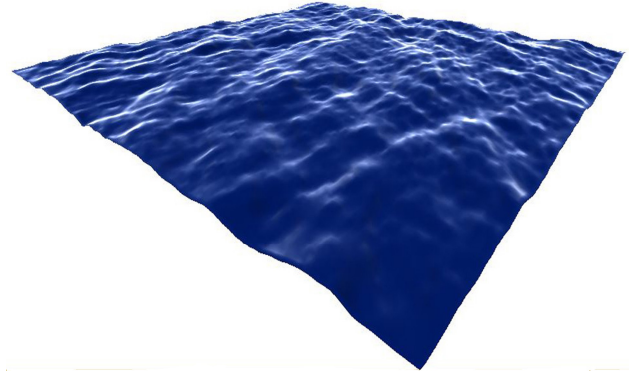
(a) $L = 256\,\mathrm{m}$

(b) $L = 512\,\mathrm{m}$

Fig. 2.   The generated ocean waves of the method of the paper ($U_{19.5} = 10.0\,\mathrm{m/s}$).

We respectively substitute the above calculated $\tilde{h}_0(\vec{k}_{ij})$ and $\tilde{h}_0(\vec{k}_{ij})$ in expression (9) and (13), and solve for $\tilde{h}(\vec{k}_{ij},t)$ and $\tilde{h}_c(\vec{k}_{ij},t)$, the Fourier coefficient. Both of the coefficients contain $\Delta s_{\vec{k}}$ and $\Psi(\vec{k}_{ij})$.

We employ the Fourier coefficient containing $\Delta s_{\vec{k}}$ and $\Psi(\vec{k}_{ij})$ to render the ocean wave, as shown in Figure 2, and get satisfactory results. As L rises, the wave shape still keeps stable.

IV. COMPARISON STUDIES

A. Comparing the Method in [18] with the Method of the Paper

P is the ocean wave potential per unit area, ρ is the water density, g is the gravity acceleration, and $P = \rho g \text{Var}(h)$. Both ρ and g are constants, so $\text{Var}(h)$ represents the potential. $\text{Var}(h)=\iint_{\vec{k}}\Psi(\vec{k})\mathbf{d}\vec{k}$, and $\Psi(\vec{k})$ is an energy spectrum.

To facilitate comparison, we respectively denote h, $\tilde{h}$, $\tilde{h}_0$ and A_{ij} in [18] by h_T, $\tilde{h}_T$, $\tilde{h}_{0,T}$ and $A_{ij,T}$. In other words, h_T, $\tilde{h}_T$ and $\tilde{h}_{0,T}$ are calculated by expression (1), (2) and (3) respectively. For the Phillips spectrum, if the expression of A includes only $A_{\Psi,Ph}$, the wave potential of the method of [18] is:

$$\text{Var}[h_T(\vec{x},t)] = \sum_{\vec{k}} \text{Var}[\tilde{h}_T(\vec{k},t)\exp(\vec{k}\cdot\vec{x})]$$
$$= \sum_{\vec{k}}[\Psi(\vec{k})+\Psi(-\vec{k})] = \sum_{\vec{k}}2\Psi(\vec{k}). \quad (20)$$

The wave potential of the method of the paper is:

$$\text{Var}[h(\vec{x},t)] = \sum_{\vec{k}}\Psi(\vec{k})\Delta s_{\vec{k}}. \quad (21)$$

So $\text{Var}[h_T(\vec{x},t)]$ does not contain $\Delta s_{\vec{k}}$, but $\text{Var}[h(\vec{x},t)]$ contains. Consequently we get below expression:

$$\begin{cases} \text{Var}[h(\vec{x},t)] = \sum_{\vec{k}}\Psi(\vec{k})\Delta s_{\vec{k}} \approx \iint_{\vec{k}}\Psi(\vec{k})\mathbf{d}\vec{k}, \\ \text{Var}[h_T(\vec{x},t)] = \sum_{\vec{k}}2\Psi(\vec{k}_{ij}) \approx \dfrac{2}{\Delta s_{\vec{k}}}\iint_{\vec{k}}\Psi(\vec{k})\mathbf{d}\vec{k}. \end{cases} \quad (22)$$

where $2/\Delta s_{\vec{k}} = (L/\sqrt{2}\pi)^2$. When the wind velocity is fixed, $\iint_{\vec{k}}\Psi(\vec{k})\mathbf{d}\vec{k}$ is a constant. In above expression, we find the $\text{Var}[h(\vec{x},t)]$ is accurate, while $\text{Var}[h_T(\vec{x},t)]$ is overlarge. What is worse, the huger L is, the larger $\text{Var}[h_T(\vec{x},t)]$ is, and the wave potential of $h_T(\vec{x},t)$ does not satisfy expression (16). So $\text{Var}[h_T(\vec{x},t)]$ is miscomputed in this case. This is the reason why the amplitude of the generated ocean wave is malformed in

Figure 1. This also explains why the malformation is turning more serious as L increases.

If the expression of A contains only $A_{\Psi,Ph}$, we find that the amplitude of the cosine wave, $A_{ij,T}$, is also miscalculated. Although [18] did not give the expression of $A_{ij,T}$, we can get it by comparison. Expression (3) is written as:

$$\tilde{h}_0(\vec{k}_{ij}) = (\varepsilon_1' + \sqrt{-1}\varepsilon_2')\sqrt{\Psi(\vec{k}_{ij})}. \quad (23)$$

where $\varepsilon_1'=\varepsilon_1/\sqrt{2}$, $\varepsilon_2'=\varepsilon_2/\sqrt{2}$, $E(\varepsilon_1')=E(\varepsilon_2')=0$ and $\text{Var}(\varepsilon_1')=\text{Var}(\varepsilon_2')=1/2$. Consequently, ε_1' and ε_2' respectively play the same role as $\cos\varphi_{ij}$ and $\sin\varphi_{ij}$. Comparing expression (23) with (10), we get $A_{ij,T}$ as:

$$A_{ij,T} = 2\sqrt{\Psi(\vec{k}_{ij})}. \quad (24)$$

The expression of $A_{ij,T}$ does not contain $\Delta s_{\vec{k}}$ either, and it is miscomputed. Hence, if L is great (i.e. $\Delta s_{\vec{k}}$ is small), $A_{ij,T} \gg A_{ij}$, and the rendered ocean wave is malformed.

The comparisons of the wave potential and the amplitude of the cosine wave indicate that the expression of A should contain not only $A_{\Psi,Ph}$.

If $\text{Var}[h_T(\vec{x},t)] = \text{Var}[h(\vec{x},t)]$ and $A_{ij,T} = A_{ij}$, A is expressed as:

$$A = \frac{1}{2}\Delta s_{\vec{k}}A_{\Psi,Ph}. \quad (25)$$

Expression (25) shows that the value of A depends on $A_{\Psi,Ph}$ as well as $\Delta s_{\vec{k}}$. In this case, both the wave potential and the amplitude of the cosine wave are computed correctly, and the shape of the generated wave is stable.

B. Comparing the Wave Potential of Open Source Codes with That of the Method of the Paper

Some well known open source codes, such as osgOcean, oceanFFT and fftrefracion, use the geometric surface to render the sea surface, i.e. the sea surface has a uniform scale of the geometric surface. So we first calculate the parameters of the geometric surface, such as the amplitude of the cosine wave and the variance of the height field, according the data of the open source code. Further we get the above-mentioned parameters of the sea surface. The aim of the comparison is to look at the difference between the potential calculated by the method of the paper and the potential of the sea surface calculated according to the open source data.

In osgOcean, the height field of the geometric surface equals to the IFFT height field. But in oceanFFT and fftrefraction, the height field of the geometric surface equals to the IFFT height field multiplied by a small factor denoted p_z. The subscripts GS and OS identify the geometric and sea surface of the open

source code respectively. Consequently, L_{GS}, A_{GS}, h_{GS} and $A_{ij,GS}$ are the length, numeric constant of the Phillips spectrum, height field and cosine wave amplitude of the geometric surface. L_{GS} and A_{GS} are given in the code. According to uniform scaling we can get:

$$p_{xyz} = \frac{L_{OS}}{L_{GS}} = \frac{h_{OS}(\vec{x},t)}{p_z h_{GS}(\vec{x},t)} = \frac{A_{ij,OS}}{p_z A_{ij,GS}}. \qquad (26)$$

where p_{xyz} is the uniform scale factor and $L_{OS} = L$. So $\text{Var}[h(\vec{x},t)] / \text{Var}[h_{OS}(\vec{x},t)]$ is express as:

$$\frac{\text{Var}[h(\vec{x},t)]}{\text{Var}[h_{OS}(\vec{x},t)]} = \left(\frac{A_{ij}}{A_{ij,OS}}\right)^2 = \left(\frac{\pi L_{GS}}{p_z L_{OS}^2}\right)^2 \frac{2A}{A_{GS}}. \qquad (27)$$

$\text{Var}[h(\vec{x},t)] / \text{Var}[h_{OS}(\vec{x},t)]$, $A_{ij} / A_{ij,OS}$ and some concerned parameters of the codes are listed in Table 1.

TABLE 1
$\text{Var}[h(\vec{x},t)] / \text{Var}[h_{OS}(\vec{x},t)]$, $A_{ij} / A_{ij,OS}$ AND CONCERNED PARAMETERS

Open source code	Concerned parameter					$\text{Var}[h(\vec{x},t)] / \text{Var}[h_{OS}(\vec{x},t)]$	$A_{ij} / A_{ij,OS}$
	$L_{OS}(L)$	L_{GS}	p_{xyz}	p_z	A_{GS}		
osgOcean	256 m	256.0	1.0	1.0	0.64×10^{-6}	1.64	1.28
oceanFFT	100 m	2.0	50.0	0.5	1.0×10^{-8}	1.10	1.05
fftrefraction	128 m	128.0	1.0	0.1	0.8×10^{-4}	0.52	0.72

In Table 1, A_{ij} and $\text{Var}[h(\vec{x},t)]$ are close to $A_{ij,OS}$ and $\text{Var}[h_{OS}(\vec{x},t)]$ respectively. So in the code of osgOcean, oceanFFT and fftrefraction, A_{GS} and p_z are adjusted to treat the amplitude malformation. The methods of adjusting A_{GS} and p_z is as effective as the method of the paper, which confirms the work of the paper.

Figure 3 is the large scale ocean scene rendered with the method of the paper. The ocean surface is constructed by 17×17 patches. The area of the patch is 256m×256m, with 128×128 IFFT grids. The program is implemented on a PC with Geforce GTX 460 GPU and Intel Core(TM) 2 Duo CPU, and the frame rate is 70 f/s. If the number of the IFFT grid of each path increases to 256×256, the frame rate is 49 f/s.

Fig. 3. The large scale ocean scene.

C. Comparing the Method of the Paper with the Method of Directly Using the Gerstner Wave

We compare the method of the paper with the method of directly using the Gerstner wave model in [6, 7, 9-14], and try other types of wave number spectra in this section.

In [6, 7, 9-14], the directional spectrum is applied to calculate the amplitude of the cosine wave. The relation between the directional spectrum and the wave number spectrum is as [36]:

$$\text{Var}(h) = \iint_{\vec{k}} \Psi(\vec{k}) d\vec{k} = \int_\omega \int_\theta E(\omega,\theta) d\omega d\theta,$$
$$\Psi(\vec{k}) = E[\omega(k),\theta] \frac{d\omega(k)}{k dk}. \qquad (28)$$

where $E(\omega,\theta)$ is the directional spectrum, $E(\omega,\theta) = S(\omega)D(\theta)$, $S(\omega)$ is the frequency spectrum and $D(\theta)$ is the directional distribution. The mostly applied $S(\omega)$ in [6, 7, 9-14] includes the P-M and JONSWAP spectra. These two frequency spectra are recommended by ITTC (International Tank Towing Conference) [38]. The widely used $D(\theta)$ is expressed as:

$$D(\theta) = \frac{1}{2\sqrt{\pi}} \frac{\Gamma(n+1)}{\Gamma(n+1/2)} \cos^{2n}\left(\frac{\theta-\alpha}{2}\right). \qquad (29)$$

where Γ is the gamma function, and n is a positive integer.

In [6, 7, 9-14], A_{ij} is expressed as:

$$A_{ij} = \sqrt{2E(\omega_i,\theta_j)\Delta s_{\omega,\theta}}. \qquad (30)$$

where $\Delta s_{\omega,\theta} = \Delta\omega\Delta\theta$. If expression (19) is used to calculate $\tilde{h}_0$, we can get below expression:

$$\text{Var}(h) = \sum_{i,j} \Psi(\vec{k}_{ij})\Delta s_{\vec{k}} \approx \sum_{i,j} E(\omega_i,\theta_j)\Delta s_{\omega,\theta}. \qquad (31)$$

One should note that in expression (31), $\Psi(\vec{k})$ is the corresponding wave number spectrum of $E(\omega,\theta)$, not only represents the Phillips spectrum. So we can arrive at the conclusion that the wave potential of [6, 7, 9-14] is very close to that of the method of the paper. To further prove the conclusion, another two wave number spectra, $\Psi_{PM}(\vec{k})$ and $\Psi_{J}(\vec{k})$, are constructed and tried.

The frequency spectrum of $\Psi_{PM}(\vec{k})$ is the P-M spectrum, and the directional distribution of $\Psi_{PM}(\vec{k})$ is in the form of expression (29) with $n = 1$. $\Psi_{PM}(\vec{k})$ is expressed as:

$$\Psi_{PM}(\vec{k}) = A_{\Psi,PM}\frac{1}{k^4}\exp\left(-\frac{\beta_{PM}g^2}{U_{19.5}^4 k^2}\right)\cos^2\left(\frac{\theta-\alpha}{2}\right).$$

(32)

where $A_{\Psi,PM} = \alpha_{PM}/2\pi$, $\alpha_{PM} = 8.1\times10^{-3}$, $\beta_{PM} = 0.74$ [38]. $\Psi_{PM}(\vec{k})$ is the spectrum of the fully developed sea. The rendering results of $\Psi_{PM}(\vec{k})$ is very similar with that of the Phillips spectrum.

The frequency spectrum of $\Psi_{J}(\vec{k})$ is the JONSWAP spectrum, and the directional distribution of $\Psi_{J}(\vec{k})$ is the same as that of $\Psi_{PM}(\vec{k})$. $\Psi_{J}(\vec{k})$ is expressed as:

$$\Psi_{J}(\vec{k}) = A_{\Psi,J}\frac{1}{k^4}\exp\left(-\frac{5}{4}\frac{\omega_{0,J}^4}{g^2 k^2}\right)\gamma^{a_J}\cos^2\left(\frac{\theta-\alpha}{2}\right).$$

(33)

where $A_{\Psi,J} = \alpha_J/2\pi$, and $\alpha_J = 0.076\bar{X}^{-0.22}$ [39], $\bar{X} = gX/U_{10}^2$, and X is the fetch,

U_{10} is the wind velocity at the height of 10 m above the sea surface,

$\omega_{0,J}$ is the peak frequency of the JONSWAP spectrum, and $\omega_{0,J} = 22(g/U_{10})\bar{X}^{-0.33}$,

γ is a constant, $1 < \gamma < 7$, with average 3.3;

$a_J = \exp[-(\omega_k - \omega_{0,J})^2/(2\sigma^2\omega_{0,J}^2)]$,

$\sigma = \begin{cases} 0.07, \text{if } \omega_k \le \omega_{0,J} \\ 0.09, \text{if } \omega_k > \omega_{0,J} \end{cases}$.

$\Psi_{J}(\vec{k})$ is used to render the developing sea. Figure 5 is the rendering results of using $\Psi_{J}(\vec{k})$ in the method of the paper. The shape of the rendered wave is stable.
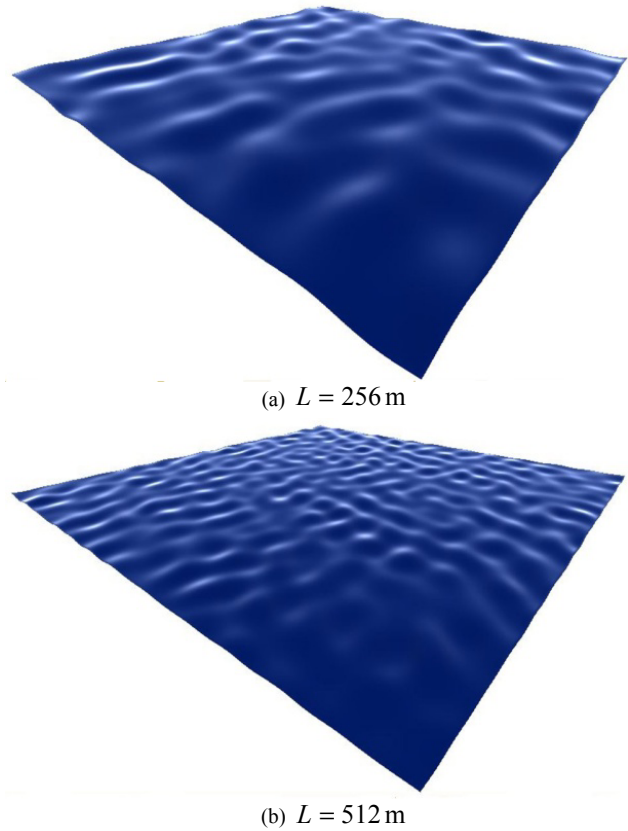

(a) $L = 256\,\text{m}$

(b) $L = 512\,\text{m}$

Fig. 5.   Rendering results of $\Psi_{J}(\vec{k})$ ($U_{10} = 11\,\text{m/s}$, $X = 50\,\text{km}$, γ=3.3).

V. HOW DO [18-30] GET GOOD RENDERING RESULTS?

Section IV provides the method of A calculating. However, in [18-30], the value of A is not mentioned. If the value of A is not proper, the amplitude of the rendered may be malformed, just as mentioned above. It confuses the author how [18-30] get satisfactory experimental results. The author infers that some factitious methods may be used to suppress the overlarge amplitude and keep wave shape stable. There are two factitious methods:

- Because A is not given, the user of the method can set A very small to keep the generated wave shape stable.
- The other method is to multiply the IFFT height field by a very small factor.

We find the authors of the three open source codes have employed such methods. osgOcean used the first, fftrefraction used the second, and oceanFFT used both. The concerned parameters are listed in Table 1. It is obvious that the code authors have already noticed the phenomenon of the amplitude malformation, but not probed the cause. Although the method is effective, it is only a matter of expediency and lack of basis. The work of the paper gives the method of A calculating, and provides theoretical basis for ocean wave rendering with the IFFT Gerstner wave model.

VI. CONCLUSIONS

Tessendorf [18] raised the model of the IFFT Gerstner wave to render the ocean wave, and [19-30] used the method. [18-30] got good rendering results. However, the value of A, a numeric constant of the Fourier coefficient, is not given in [18-30]. The shape of the rendered ocean wave is under the influence of A. If the value of A is not proper, the amplitude of the generated wave is malformed, and the larger the rendered sea surface, the more serious the malformation. So the author thinks that the method in [18] need be re-examined and the method of A calculating should be provided.

The expression of the IFFT Gerstner wave with the amplitude of the cosine wave is re-derived at first. Then the right Riemann sum is used to discretize the definite integral of the wave number spectrum, and the area of the discrete integral domain is determined by the sample mode for the wave number vector in IFFT. Further we get the expression of the IFFT Gerstner wave, and the Fourier coefficient of the expression contains the wave number spectrum and area of discrete integral domain. The method mentioned above treats the amplitude malformation and keeps the generated wave form stable.

Comparison studies and experiments are done to calculate the value of A and approve the value.

By comparing the expression of the method of the paper with that of [18], we find that the expression of A should contain not only $A_{\Psi,Ph}$, the spectral constant of the wave number spectrum of the Phillips spectrum, but also $\Delta s_{\bar{k}}$, the area of discrete integral domain of the sampled wave number vector. If the expression of A contains only $A_{\Psi,Ph}$, the potential of the rendered wave is overlarge, and the amplitude malformation occurs. The larger the width of the rendered sea surface, the more serious the malformation. If the expression of A contains $A_{\Psi,Ph}$ and $\Delta s_{\bar{k}}$, both the wave potential and the amplitude of the cosine wave are correctly calculated, and the shape of the generated wave is stable.

After reading some well known open source codes, including osgOcean, oceanFFT and fftrefraction, we find the code authors take factitious methods to suppress the amplitude malformation, and the wave potential of the suppressed wave is close to that of the method of the paper. It is obviously appeared that the code authors have already noticed the phenomenon of the amplitude malformation, but not discovered the cause. The factitious method is effective, but lack of basis. In the author's opinion, the factitious method is the reason why [18-30] achieve good results.

We compare the method of directly using the Gerstner wave with the method of the paper. In the former method, the directional spectrum is used to calculate the amplitude of the cosine wave. The wave potential of the method is quite close to that of the method of the paper. The P-M and JONSWAP spectra are employed to construct another two wave number spectra respectively. Both shapes of the rendered wave are stable.

The comparisons and experiment results show that the method of the paper can precisely compute the wave potential, and effectively correct the amplitude malformation.

The wave spectrum used in the above mentioned references, either the wave number spectrum or directional spectrum, is the spectrum of the wind sea. So the generated wave is the wind sea. The wind sea spectrum is reasonably accurate for sever states. However, moderated and low sea states are often of combined nature, consisting of both wind sea and sea swell [40]. So the future work may concentrate in the rendering of the mixed wave and the sea swell. The mixed wave includes the wind sea as well as the sea swell. To animate the mixed wave, we may try the two peak spectrum [40, 41]. The swell spectrum [42] can be applied in rendering the sea swell. This work will make the rendered ocean wave more realistic.

REFERENCES

[1] S. Bruce, "Long crested wave models," *Computer Graphics and Image Processing*, Vol. 12, No. 2, pp. 187-201, Feb. 1980.

[2] M. Nelson, "Vectorized procedural models for natural terrain: wave and islands in the sunset," *Computer Graphics (ACM)*, Vol. 15, No. 3, pp. 317-324, Aug. 1981.

[3] A. Osborne, *Nonlinear ocean waves and the inverse scattering transform*. Boston, USA: Academic Press, 2010, pp. 3-10.

[4] A. Craik, "The origins of water wave theory," *Annual Review of Fluid Mechanics*, Vol. 36, pp. 1-28, Jan, 2004.

[5] A. Fournier and W. Reeves, "A simple model of ocean waves," *Computer Graphics (ACM)*, Vol. 20, No. 4, pp. 75–84, Aug, 1986.

[6] S. Thon and D. Ghazanfarpour, "Ocean waves synthesis and animation using real world information," *Computers & Graphics*, Vol. 26, No. 1, pp. 99-108, Feb. 2002.

[7] J. Fréchot, "Realistic simulation of ocean surface using wave spectra," in *Proceedings of the 1st International Conference on Computer Graphics Theory and Applications (GRAPP' 06).*, Setubal, Portugal, 2006, pp. 76-83.

[8] E. Darles, B. Crespin, D. Ghazanfarpour, and J. Gonzato, "A survey of ocean simulation in computer graphics," *Computer Graphics Forum*, Vol. 30, No. 1, pp. 43-60, Mar, 2011.

[9] D. Hinsinger, F. Neyret and M. Cani. "Interactive animation of ocean waves", in *Proceedings of the 1st ACM SIGGRAPH / Eurographics Symposium on Computer Animation (SCA' 02)*, New York, USA, pp. 161-166, 2002.

[10] E. Darles, B. Crespin, and D. Ghazanfarpour, "Accelerating and enhancing rendering of realistic ocean scenes," in *Full Paper Proceedings of the 15th International Conference in Central Europe on Computer Graphics, Visualization and Computer Vision (WSCG' 07), Part 2*, Plzen, Czech, 2007, pp. 287-294.

[11] X. Zhao, F Li, H. Chen , and S. Zhan, "Ocean wave simulation near the seashore," *Journal of Beijing Institute of Technology*, Vol. 18, No. 2, pp. 181-185, Jun. 2009.

[12] G. Yin, H. Wang, J. Zhang, H. Chen, "Fractal reconciliation for ocean wave simulation," *Journal of Harbin Engineering University*, Vol. 32, No. 11, pp. 1495-1500, Nov. 2011.

[13] S. Liu and W. Zhang, "Cartoon-style simulation of water coupled with objects," *Simulation Modeling Practice and Theory*, Vol. 32, No. 2, pp. 52-62, Feb. 2013.

[14] K. Prachumrak and T. Kanchanapornchai. "Real-time interactive ocean wave simulation using multithread," *World Academy of Science, Engineering and Technology*, Vol. 5, pp. 235-238, Aug. 2011.

[15] R. Bridson, *Fluid simulation for computer graphics*. Wellesley, MA, USA: A K Peters, Ltd., 2008, pp. 187-194.

[16] D. Wu, X. Zou, K. Dai et al, "Implementation and evaluation of parallel FFT on Engineering and Scientific Computation Accelerator (ESCA) architecture," *Journal of Zhejiang University – Science C (Computers & Electronics)*, Vol. 12, No. 12, pp. 976-989, Dec. 2011.

[17] J. Lobeiras, M. Amor, and R. Doallo, "FFT implementation on a stream architecture," in *Proceedings of the 19th International Euromicro*

Conference on Parallel, Distributed, and Network-based Processing (PDP' 11)., Ayia Napa, Cyprus, 2011, pp. 119-126.

[18] J. Tessendorf (1999, Aug). Simulating ocean water [Online]. Available: http://graphics.ucsd.edu/courses/rendering/2005/jdewall/tessendorf.pdf

[19] H. Ren, Y. Yin, and Y. Jin, "Realistic rendering of large-scale ocean wave scene," *Journal of Computer-Aided Design and Computer Graphics*, Vol. 12, No. 12, pp. 1617-1622, Dec. 2008.

[20] C. Christie, E. Gouthas, L. Swierkowski and O. Willianms, "Real-time maritime scene simulation for ladar sensors," in *Proceedings of SPIE, Vol. 8015*, Orlando, USA, pp. G1-G12, 2011.

[21] J. Mitchell. "Real-time synthesis and rendering of ocean water," ATI Research Technical Report, Marlboro, USA, Apr. 2005.

[22] E. Miandji, M. Sargazi Moghadam, F. Samavati and M. Emadi, "Real-time multi-band synthesis of ocean water with new iterative up-sampling technique," *Visual Computer*, Vol. 25, No. 5-7, pp. 697-705, May. 2009.

[23] L. Swierkowski, E. Gouthas, C. Christie and O. Williams, "Boat, wake and wave real-time simulation," in *Proceedings of SPIE, Vol. 7031*, San Diego, USA, pp. A1-A12, 2009.

[24] M. Weerasinghe, D. Sandaruwan, C. Keppitiyagama, and N. Kodikara, "A novel approach to simulate wind-driven ocean waves in the deep ocean," in *Proceedings of the 13th International Conference on Advances in ICT for Emerging Regions (ICTER' 13)*, Colombo, Sri Lanka, pp. 28-37, 2013.

[25] S. Wang, F. Kang, and D. Wang, "Ocean wave real-time simulation based on adaptive fusion," in *Proceedings of the 32nd Chinese Control Conference (CCC' 13), Xi'an, China*, pp. 26-28, 2013.

[26] M. Nielsen, A. Söderström, and R. Bridson, "Synthesizing waves from animated height fields," *ACM Transactions on Graphics*, Vol. 32, No. 1, pp. 2:1-2:9, Jan. 2013.

[27] Y. Chiu, and C. Chun, "GPU-based ocean rendering," in *Proceedings of the 7th International Conference on Multimedia and Expo (ICME' 06)*, Toronto, Canada, pp. 2125-2128, 2006.

[28] C. Wang, J. Wu, C. Yen, P. Liu and C. Chen, "Ocean wave simulation in real-time using GPU," in *the 38th International Computer Symposium (ICS' 10)*, Tainan, Taiwan, pp. 419-423, 2010.

[29] T. Grindstad and R. Rasmussen, "Deep water ocean surface modeling with ship simulation", M. S. Thesis, Dept. Marine Technology, Norwegian University of Science and Technology, Trondheim, Norway, 2011.

[30] L. Zhang, C. Guo, Y. Tang, M. Lv, Y. Li and J. Zhao. "Real-time and realistic simulation of large-scale deep ocean wave foams based on GPU,"

Journal of Computational Information Systems, Vol. 10, No. 7, pp. 2821-2828, Apr. 2014.

[31] B. Kim (2009). osgOcean 1. 0. 1 [Online]. Available: http://code.google.com/p/osgocean/

[32] NVIDIA (2013). oceanFFT, examples of CUDA toolkit [Online]. Available: https://developer.nvidia.com/cuda-toolkit

[33] J. Dart (2003). fftrefraction [Online]. Available: http://www.pudn.com/downloads346/sourcecode/windows/opengl/detail 1510268.html

[34] O. Phillips. "The equilibrium range in the spectrum of wind-generated waves," *Journal of Fluid Mechanics*, Vol. 4, No. 4, pp. 426-434, Aug. 1958.

[35] L. Chen, Y. Jin, Y. Yin and H. Ren, "On the wave spectrum selection in ocean wave scene simulation of the maritime simulator," in *Communications in Computer and Information Science, Vol. 402*, pp. 453-465.

[36] COST Action 714 Working Group 3. *Measuring and analyzing the directional spectrum of ocean waves*. Luxembourg: Office for Official Publications of the European Communities, 2005, pp. 16-20, 40-46.

[37] M. Weir, J. Hass, and F. Thomas, *Thomas' calculus including second-order differential equations (11th Edition)*, Boston, USA: Pearson Addison - Wesley, 2006, pp. 603-610.

[38] Specialist Committee on Waves, "Final report and recommendations to the 23rd ITTC," in *Proceedings of the 23rd ITTC, Vol. 2*, Venice, Italy, pp. 545-547, 2002. Available: http://ittc.sname.org/proc23/Waves.pdf

[39] Y. Yu and S. Liu. *Random wave and its applications to engineering (4th Edition)*. Dalian, China: Dalian University of Technology Press, 2011, pp. 149-152.

[40] E. Bitner-Gregersen and O. Hagen, "Directional spreading in two-peak spectrum at the Norwegian continental shelf," in *Proceedings of the 21st International Conference on Offshore Mechanics and Arctic Engineering (OMAE' 02), Vol. 2*, Oslo, Norway, pp. 547-556, 2002.

[41] K. Torsethaugen and S. Haver, "Simplified double peak spectral model for ocean waves." in *Proceedings of the 14th International Offshore and Polar Engineering Conference (ISOPE' 04)*, Toulon, France, pp. 76-84, 2004.

[42] M. Olagnon, K. Kpogo-Nuwoklo. and Z. Guede, "Statistics processing of West Africa wave directional spectra time-series into a climatology of swell events," *Journal of Marine Systems*, Vol. 130, pp. 101 -108, Feb, 2014.